

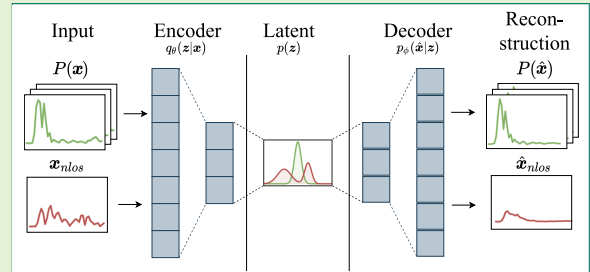
# Estimating TOA Reliability with Variational Autoencoders

Maximilian Stahlke, Sebastian Kram, Felix Ott, Tobias Feigl, and Christopher Mutschler

**Abstract**—Radio frequency (RF)-based localization yields centimeter-accurate positions under mild propagation conditions. However, propagation conditions predominant in indoor environments (e.g. industrial production) are often challenging as signal blockage, diffraction and dense multipath lead to errors in the time of flight (TOF) estimation and hence to a degraded localization accuracy. A major topic in high-precision RF-based localization is the identification of such anomalous signals that negatively affect the localization performance, and to mitigate the errors introduced by them. As such signal and error characteristics depend on the environment, data-driven approaches have shown to be promising. However, there is a trade-off to a bad generalization and a need for an extensive and time-consuming recording of training data associated with it.

We propose to use generative deep learning models for out-of-distribution detection based on channel impulse responses (CIRs). We use a Variational Autoencoder (VAE) to predict an anomaly score for the channel of a TOF-based Ultra-wideband (UWB) system. Our experiments show that a VAE trained only on line-of-sight (LOS) training data generalizes well to new environments and detects non-line-of-sight CIRs with an accuracy of 85%. We also show that integrating our anomaly score into a TOF-based extended Kalman filter (EKF) improves tracking performance by over 25%.

**Index Terms**—NLOS identification, NLOS mitigation, channel quality estimation, CIR, UWB, Deep Learning, VAE.



## I. INTRODUCTION

High precision radio frequency (RF) localization enables many indoor applications including the monitoring of production facilities or robot localization. Technologies such as Wi-Fi [1], Bluetooth [2], RFID [3], and Ultra wideband (UWB) have been developed and optimized over recent years [4] to achieve this. In contrast to most localization systems that yield localization accuracies in the meter or decimeter range, UWB uses a high bandwidth to estimate positions in the centimeter range. However, this requires optimal signal propagation conditions with a line of sight (LOS) between transmitters and receivers, which can only rarely be found in (industrial) environments. Enabling high positioning accuracy in the presence of multipath propagation, especially under non-line-of-sight (NLOS), is among the main research challenges.

UWB systems often use the time-of-flight (TOF) to obtain range-estimates between transmitters and receivers. A downstream multi-lateration or tracking filter estimates the positions

Submitted March, 30th 2021, revised XX-XX-XXXX, published XX-XX-XXXX. This work was supported by the Bavarian Ministry of Economic Affairs, Infrastructure, Energy and Technology as part of the Bavarian projects Leistungszentrum Elektroniksysteme (LZE) and the Center for Analytics-Data-Applications (ADA- Center) within the framework of "BAYERN DIGITAL II".

Maximilian Stahlke, Sebastian Kram, Felix Ott, Tobias Feigl and Christopher Mutschler are with the Fraunhofer Institute for Integrated Circuits IIS, Nuremberg, Germany (e-mails: firstname.lastname@iis.fraunhofer.de).

Tobias Feigl and Sebastian Kram are also with the Friedrich-Alexander University Erlangen-Nürnberg (FAU).

of the transmitters. Fig. 1 shows propagation scenarios from indoor environments that potentially lead to wrong range estimates. The green line shows an LOS path from TX to RX<sub>4</sub> while the red paths show signal propagation paths with a different length from their actual distance due to reflection (RX<sub>1</sub>), diffraction (RX<sub>2</sub>), obstruction (RX<sub>3</sub>), and scattering (RX<sub>4</sub>). The indirect path caused by reflections usually leads to a significant bias  $\Delta d$ . Note that even under LOS propagation, multipath components (MPC) may lead to erroneous estimates due to bandwidth and signal power limitations. MPCs can overlap with the direct path and a lower signal to noise ratio

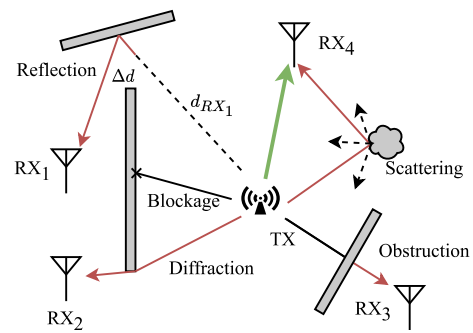


**Fig. 1:** Complex propagation conditions, including specular reflections, scattering, blockage and diffraction; gray rectangles are walls and arrows are signal propagation paths from the transmitter TX to the receivers RX<sub>1</sub> to RX<sub>4</sub>.

(SNR) leads to a degrading distance estimation [5].

Classical position estimators (such as least squares optimizers or Bayesian tracking filters) suffer from such biased range estimates. This is why a binary (LOS and NLOS) signal classification often helps to mitigate the impact on the localization performance [6]. As the propagation conditions strongly depend on the environment, data-driven approaches have so far achieved the most promising results in NLOS identification [7]. For the categorization of TOF signals often the channel impulse response (CIR) serves as a basis as it contains a variety of spatial information about the environment and its propagation conditions [8]. On the downside, as such signals are highly environment-dependent [9], data-driven methods to detect NLOS CIRs often do not generalize well to different environments (i.e., the shape of the NLOS CIRs is directly influenced by the geometry of the environment).

To bypass this generalization problem our main idea is to only use LOS CIRs for training, as we assume that LOS CIRs are less influenced by the environment, as the direct path is the crucial aspect in the CIR. This also makes the deployment easier and leads to a better generalization in contrast to the related approaches which need both classes for training (as they need a representative dataset). Our idea is to model the distribution of normal samples (i.e., LOS signals with reliable TOF estimates) to identify out-of-distribution signals (i.e., signals with significant TOF errors) using a variational autoencoder (VAE) (i.e., a deep learning based generative model). Instead of estimating anomaly categories we predict a continuous quality parameter that enables a more detailed rating of the input signals in the downstream processing. Our experiments with real world CIRs from a UWB-system not only show that we outperform existing *one-class and unsupervised* approaches in the detection of NLOS CIRs but that we also can considerably improve the tracking accuracy in a challenging mixed environment (with our algorithm only trained in a pure LOS environment).

The remainder of this article is structured as follows. Sec. II reviews related work before Sec. III provides details about our method. We describe the experimental setup in Sec. IV and discuss the results in Sec. V.

## II. RELATED WORK

### A. Anomaly identification

While anomalous or erroneous signals have different levels of degradation, the problem is often simplified to a binary classification that only considers LOS and NLOS signals. While there are approaches that analyze the CIRs on a coarse grain (e.g., Kolakowski et al. [10] assume that NLOS signals are more attenuated than LOS signals and use a threshold on the maximum power) most approaches extract features from the CIRs and use them for an ML-based classification.

Very popular is the usage of Support Vector Machines (SVMs) [11]. However also a decision tree classifier has been used [12]. In contrast to most NLOS identification approaches that only consider two classes (LOS/NLOS) there is also work that considers a more fine-grained categorization [13], [14].

In contrast to ML-based approaches that require a manual feature extraction (which restricts them in the expressive power

of used features), models based on deep learning (DL) directly work on raw data. Their modeling of the predominant nonlinearities shows promising results for e.g. direct positioning from CIRs [15], [16] or velocity estimation [17]. Such methods have also been used in the context of NLOS identification where even small networks outperform existing approaches [7]. Related DL-based approaches use deep feed forward networks on the power of the first component [18], short-time Fourier transform of the CIR in a convolutional neural network (CNN) as a 2D image [19], or combine CNN-based feature extraction with long short-term memory (LSTM) architectures to model time dependencies in the signals [20]. However, all these approaches (including those that use transfer learning [21]) need representative data of both LOS and NLOS CIRs.

There is also work much closer to ours that also only relies on LOS CIRs for training. Zeng et al. [22] compare a set of reference LOS CIRs with the test set using a Pearson correlation coefficient to get a reliability score. Miao et al. [9] employ a one-class SVM that identifies the smallest hypersphere including all normal data (i.e., LOS CIRs) to implicitly classify NLOS (which is supposed to be not included in the hyper-sphere). Fan et al. [23] use a unsupervised feature based approach, which uses expectation-maximization to model a Gaussian mixture model (GMM) to identify clusters for LOS and NLOS in an unlabeled dataset. In contrast to them, we exploit the raw CIR in a VAE to model the distribution of LOS CIRs. This leads to a richer representation of our normal data and therefore to a better identification of abnormal samples.

### B. Anomaly mitigation

To exploit identified NLOS signals in positioning we can either (1) exclude them (which, however, only works when a sufficient number of receivers with LOS will still be available) or we can (2) reuse them by correcting their ranging bias.

Maranò et al. [24] propose a least-squares SVM NLOS identification to exclude NLOS signals. If there are less than three nodes available the biases of the NLOS signals are estimated and subtracted from the estimated ranges. Such frameworks can also be realized with different classifiers such as k-nearest neighbor [25]. There is also work that skips the identification and immediately corrects the bias, e.g. through Gaussian processes [26]. Wang et al. [27] used a semi-supervised SVM to exploit unlabeled measurements, with only a small subset of labeled samples, for range error mitigation.

While those approaches use features extracted from the CIRs also DL-based approaches have been proposed. Schmid et al. [28] employ the range and features of the signal in a feed-forward neural network that estimates the bias of the estimated range. Bregar et al. [29] exploit the raw CIR to regress the error through a CNN.

Another class of approaches models uncertainties for range estimates based on a channel model with known channel statistics [30] or by modeling *soft* ranges [31] (i.e., a list of range estimates with associated likelihoods). Mao et al. [32] propose a Bayesian neural network for range error estimation with uncertainty quantification. However, those approaches require extensive measurement campaigns for sensing channel information and ground truth positions.

All such approaches require extensive measurement data: NLOS identification requires a database with signal information of LOS and NLOS labels while richer reliability representations require channel states and ground truth positions. In contrast, our approach is only trained on LOS CIRs to estimate a continuous anomaly score that can not only be used for NLOS identification but also to estimate the bias and variance in a Kalman filter to enhance the tracking performance.

### III. METHODOLOGY

For TOF-based positioning system we consider signals to be anomalous if they induce perceptible TOF estimation errors that degrade the localization performance. Hence, our idea is to approximate the distribution of normal signals (LOS signals from which we can reliably estimate the TOF) to identify abnormal signals as *out-of-distribution* samples.

Moreover, instead of only categorizing the signals we aim at estimating a continuous quality parameter that enables a more fine-grained processing of the signals in downstream tasks (such as positioning).

#### A. ML-based Anomaly Detection

Anomaly detection is often used on tasks in which we have plenty of data from *normal* situations while data from *abnormal* situations is rare. Classical ML-based approaches such as Bayesian networks, one-class (OC) SVMs, or k-nearest neighbors have successfully been applied for anomaly detection [33]. However, their requirement of a low-dimensional feature input needs a feature extraction which is not trivial to obtain and often leads to information loss.

Hence, DL approaches have recently been investigated. Such approaches include one-class neural networks (OC-NN) [34] (similar to OC-SVMs) or OC-NNs with feature inputs from a pre-trained CNN together with pseudo-negative samples from a Gaussian [35]. Beside end-to-end models (that directly perform a classification) generative approaches became popular recently. They model the distribution of normal samples to identify abnormal out-of-distribution samples. For instance, generative adversarial networks (GANs) [36] model the distribution of a latent space in an adversarial way to detect abnormal input [37], [38]. However, as GANs are difficult to stabilize during training [39] approaches based on variational autoencoders (VAEs) are often used instead as they also allow to model such distributions [40]. Sampling from the estimated latent space of the input allows to determine a mean reconstruction error that is higher for abnormal samples.

#### B. The Variational Autoencoder (VAE)

Variational autoencoders (VAEs) have been demonstrated to learn structured latent representations of high dimensional data [41]. A VAE consists of an encoder  $q_\theta$ , which maps input data samples to latent distributions, and a decoder  $p_\phi$ , which maps latent variables to distributions over data points. The parameters of the encoder and decoder,  $\theta$  and  $\phi$  respectively, are jointly trained to maximize

$$\mathcal{L}(\phi, \theta; x, z) = \mathbb{E}_{q_\theta(z|x)} [\log p_\phi(x|z)] - \beta D_{KL}(q_\theta(z|x) || p(z))$$

where  $p(z)$  is some prior (which we take to be the unit Gaussian) and  $D_{KL}$  is the Kullback-Leibler divergence. In this work we use the the beta-VAE [42], a extension of the original VAE objective with a hyperparameter  $\beta$  that balances the data-likelihood and the latent distribution constraint. The encoder  $q_\theta$  parameterizes the mean and log-variance diagonal of a Gaussian distribution,  $q_\theta(z) = \mathcal{N}(\mu(z), \sigma_\theta^2(z))$ . The decoder  $p_\theta$  parameterizes a Bernoulli distribution for each value in the raw observation. This parameterization corresponds to training the decoder with cross-entropy loss on a raw observation input.

#### C. VAE-based Anomaly Detection

Our approach uses the aforementioned VAE to detect anomalous signals. The advantage of using the VAE is that it allows us to map high-dimensional data samples  $x_i$  from a complex and unknown distribution  $P(x)$ , i.e.,  $x_i \sim P(x)$ , into a (lower-dimensional) space on which we define a distribution  $P(z)$  using neural networks and variational inference.

We define each individual CIR  $x_i$  as a complex vector  $x_i = [x_1, \dots, x_{N_s}]^T$ , with  $P(x)$  being the (unknown) data distribution over all observed LOS CIRs. The figure in the abstract shows the structure of our VAE. The encoder is used to estimate a conditional probability density function (PDF)  $q_\theta(z|x_i)$  for a given  $x_i$  in a latent space whose dimensionality can be chosen arbitrarily but that is usually much smaller than the input space. The decoder then performs an inverse transformation of a sample  $z_i \sim q_\theta(z|x_i)$  under the condition that  $x_i \approx \hat{x}_i$ . The distribution  $p(z)$  of the latent variables are often chosen to be simple, in our case as isotropic Gaussian  $p(z) \sim \mathcal{N}(0, I)$ , where  $I$  is the unit matrix. To optimize the VAE for an arbitrary  $p(x)$ ,  $\theta$  and  $\phi$  are optimized using a sufficient number of samples drawn from  $P(x)$ , see [41].

Our preliminary experiments suggest feed-forward neural networks with three layers of (100, 80, 60) and (60, 80, 100) neurons in the encoder and decoder, and two latent variables. This configuration yields a good trade-off between computation time, accuracy, overfitting and generalization.

After optimizing the VAE on the training data distribution  $P(x)$  that only consists of LOS CIRs, the decoder is able to both sample and reconstruct CIRs from this distribution well. Abnormal samples (such as NLOS CIRs) do not lie within the training data distribution  $P(x)$  and are mapped to latent variables from which a reconstruction performs poorly.<sup>1</sup>

#### D. Log-Likelihood Metrics for CIR-Reconstruction

The objective function of the VAE has two parts: (1) the log-likelihood of the data (i.e., the reconstruction error) and (2) a regularization term that constrains the latent distribution towards the target distribution (i.e., that enforces zero-mean Gaussian distributions of the latent variables). While the

<sup>1</sup>Note that also a batch of NLOS signals as input to the trained VAE results in a latent space that is not well aligned to a unit Gaussian. While we could also exploit this to detect *out-of-distribution* samples we focus on the reconstruction as this allows to evaluate single samples (instead of batches).

second term works well for our problem we need to find an appropriate metric that measures the data likelihood.

The metrics are defined for an arbitrary one-dimensional input vector  $\mathbf{y}$  and its reconstruction  $\hat{\mathbf{y}}$ . We investigate three candidates to measure the similarity of the observed and reconstructed CIRs: (1) the mean-squared error, (2) the Pearson correlation coefficient, (3) the time index signal strength indicator.

1) *Mean squared error*: A typical and widely used metric (also in VAEs) is the mean squared error (MSE). The MSE considers the quadratic error of the signals at any time index:

$$\text{MSE}(\mathbf{y}, \hat{\mathbf{y}}) = \frac{1}{N} \sum_{n=1}^{N_s} (y[n] - \hat{y}[n])^2. \quad (1)$$

However, while being a metric that is easy to optimize, the MSE is more sensitive to large errors, as the errors are squared (in contrast to metrics such as the mean absolute error). For the evaluation, we normalize both the input and reconstructed CIR with the maximum of the input CIR to make the metric insensitive to different amplitude levels of the signals.

2) *Pearson correlation coefficient*: The Pearson correlation coefficient (PCC) measures the linear correlation between two random variables. It is well-known as a distance metric for time series clustering [43]. The discrete PCC is defined as

$$r(\mathbf{y}, \hat{\mathbf{y}}) = \frac{\sum_{n=1}^{N_s} (y[n] - \bar{y})(\hat{y}[n] - \bar{\hat{y}})}{\sqrt{\sum_{n=1}^{N_s} (y[n] - \bar{y})^2} \sqrt{\sum_{n=1}^{N_s} (\hat{y}[n] - \bar{\hat{y}})^2}}, \quad (2)$$

where  $\bar{y}$  and  $\bar{\hat{y}}$  are the means of  $\mathbf{y}$  and  $\hat{\mathbf{y}}$ .

3) *Time index signal strength indicator*: As the aforementioned metrics only consider the similarity of time series in general we define a metric that also takes the semantic similarity of CIRs into account. We assume that (1) the VAE reconstructs all valid LOS signal components within the CIR well while invalid signal components only remain with a small magnitude in the reconstructed CIR, and (2) that a high signal to noise ratio (SNR) is more reliable for TOF estimation [5]. Hence, large magnitudes are more likely to be valid than smaller ones. We therefore use the Time Index Signal Strength Indicator (TISSI) to weight the input signal components with the reconstructed signal components at any time index:

$$\text{TISSI}(\mathbf{y}, \hat{\mathbf{y}}) = \sum_{n=1}^{N_s} (|y[n]| \cdot |\hat{y}[n]|). \quad (3)$$

The sum of all valid signal components is therefore a good indicator on how anomalous an input signal is. While TISSI is not a distance metric, i.e., we cannot use it for training, it offers advantages for testing, see Sec. V-A.

### E. Deriving the Anomaly Score

We use the reconstruction error as a measure of anomaly. As the latent space representation of each individual CIR  $\mathbf{x}_i$  is represented by a Gaussian distribution in the VAE from which  $N_k$  individual latent space representation  $z_{i,j}$  are sampled (i.e.,  $z_{i,j} \sim P(\mathbf{z}|\mathbf{x}_i)$ ), the reconstructed CIR is obtained by

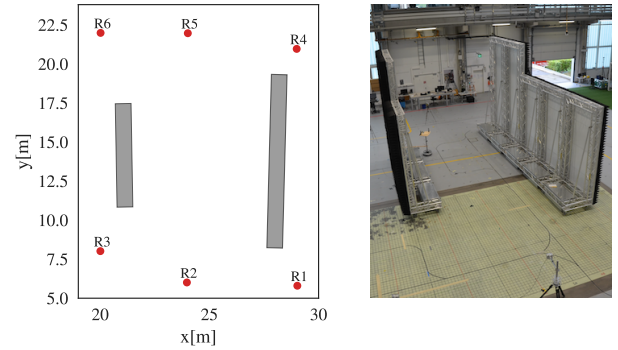


Fig. 2: Schematic top view (left) of the corridor environment (right). Grey rectangles are reflective walls; red dots show the receivers R1-R6.

applying the decoder on  $z_i$ , so that  $\hat{\mathbf{x}}_{i,j} = q_\theta(z_{i,j})$ . Based on the reconstruction, we calculate the anomaly score by

$$\Psi(\mathbf{x}_i) = \frac{1}{N_k} \sum_{j=1}^{N_k} \mathcal{L}(\mathbf{x}_i, \hat{\mathbf{x}}_{i,j}), \quad (4)$$

where  $\mathcal{L}$  is one of the distance metrics introduced in Sec. III-D. From experiments we found that drawing  $N_k \geq 10$  yields reliable results. With the definition above we assume that samples with a higher anomaly score induce larger ranging errors.

### F. Tracking filter integration of anomaly score

As the anomaly score can be related to both a systematic bias in the TOF estimation and an increased estimation uncertainty, it can be included into the observation model of an extended Kalman filter (EKF). Using the anomaly score to estimate a TDOA bias  $b(\Psi_n)$  for each TDOA  $n$ , the measurement model can be adapted to

$$h_n(\mathbf{x}) = d_n(\mathbf{x}) - d_0(\mathbf{x}) + b(\Psi_n) \quad \forall n \in [1, \dots, N_r], \quad (5)$$

where  $d_n(\mathbf{x})$  and  $d_0(\mathbf{x})$  denote the distances to receiver  $n$  and the reference receiver 0. As  $b(\Psi)$  is independent of  $\mathbf{x}$ , the linearized measurement function is not affected by this addition. The anomaly score can also be seen as a stochastic quality indicator and hence used for the definition of the measurement covariance matrix  $\mathbf{R}$ , s.t. an error variance  $\sigma^2(\Psi)$  can be assumed for each receiver  $n$ . From the assumption that the measurement noise in the TDOAs is stochastically independent follows the measurement covariance matrix:<sup>2</sup>

$$\mathbf{R} = \text{diag}([\sigma^2(\Psi_1), \dots, \sigma^2(\Psi_{N_r})]). \quad (6)$$

We show the estimation of  $b(\Psi)$  and  $\sigma^2(\Psi)$  for an exemplary tracking problem in our experimental results in Sec. V-B.

<sup>2</sup>Our model does not consider the statistical dependence of the error terms, which is introduced by the addition of the uncertainty in determining  $d_0(\mathbf{x})$ . However, under the assumption that anchor 0 has pure LOS this term is significantly smaller than the error terms occurring in NLOS conditions.

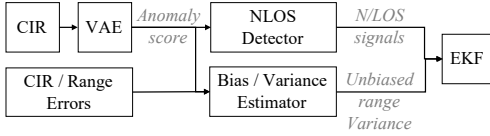


Fig. 3: Training and evaluation pipeline.

#### IV. EXPERIMENTAL SETUP

We evaluate our anomaly detection by investigating the tracking performance of a time-difference-of-arrival (TDOA) based Kalman filter. This shows the applicability and the generalization of the algorithm. We evaluate tracking in a complex environment with NLOS and dense multipath propagation, while we train our anomaly detection in a clean scenario that only contains LOS conditions and low multipath propagation.

##### A. Environments

Our training environment is an ideal positioning scenario with LOS connections between all receivers and transmitters. There are no obstacles close to the recording area of size 45 m x 25 m. Ground, walls and ceiling only induce marginal multipath propagation. The scenario includes 6 different receivers, which are placed around the recording area, shown as red dots, see Fig. 2.

In a second step we add reflective walls systematically within the area to create mixed (LOS / NLOS) propagation conditions. The walls are aligned as a corridor, which allows to easily label the data as (LOS / NLOS) geometrically, using the position of the receivers and the walls.

We recorded 198,461 LOS CIRs in the clean scenario, and 262,133 LOS CIRs and 42,765 NLOS CIRs in the corridor environment.

##### B. Hardware setup

Our 6 stationary receivers and the moving transmitter use a Decawave DW1000 UWB transceiver module. We configured a TDOA setup and recorded the TDOAs and CIRs for each of the receivers. We used a fixed receiver under good LOS conditions as a reference receiver. The TDOAs and their associated CIRs are recorded with a sampling rate of 10 Hz. A high precision optical Nikon iGPS localization system delivers ground truth positions at a positional error <1 mm.

#### V. EVALUATION

Erroneous TOF estimates harm localization accuracy as estimators such as Kalman Filters rely on constant variance and unbiased range estimations. In literature, two different approaches are proposed to enhance localization accuracy in mixed (LOS / NLOS) environments using tracking filters or least squares optimizers: (1) excluding all NLOS CIRs, or (2) correcting their error to make them usable again. We show that we enable both (1) an NLOS identification and (2) an estimation of error variance and bias to enhance the tracking performance of a TOF-based extended Kalman filter (EKF).

Fig. 3 shows our training and evaluation pipeline. We first train the VAE only on LOS CIRs. To then classify between

NLOS and LOS we pick a threshold on the anomaly score (that we can either tune manually or automatically with validation data). We discuss the results of the NLOS identification in Sec. V-A. Sec. V-B shows how to estimate the TOF bias and variance for the EKF (with additional data including CIRs and their ranging errors) and evaluates the tracking performance.

##### A. NLOS identification

To evaluate the NLOS identification performance we use the clean and corridor environment. We split the training data set into a training and validation subset and use a balanced test data set, separate from the training and validation data. The CIR contains 60 samples at a resolution of 1 ns with a real and an imaginary part that we (1) concatenate to a 120 samples long input tensor and (2) normalize (use absolute values and a scaling to get values between 0 and 1) to facilitate the optimization for the VAE.

1) *Baselines*: We used four approaches known from literature that serve as a baseline to compare our approach with.

**CORR** [22] estimates the Pearson correlation coefficient with a set of reference LOS CIRs. We use the magnitude of the CIR and 110 samples starting 10 samples before the main peak. As reference CIRs, 100 randomly LOS CIRs were chosen from the training database. We use the estimated mean Pearson correlation coefficient as a reliability score for the given CIRs of the test dataset.

**GMM** [23] and **OC-SVM** [9] are both ML-based baselines. We used six features: energy index, correlation maximum, energy decay time index, peak decay exponent and spectral features (bandwidth, centroid, rolloff, flatness). On the time-frequency features we applied a principal component analysis and only used the two main components. We optimized the hyper-parameters of the OC-SVM with a grid search<sup>3</sup>. As GMMs assume that all features follow Gaussians, we evaluated all possible features combinations as inappropriate distributed features lead to a degrading classification performance.

A **GAN** [44], a deep generative model, with an encoder  $E(x)$ , a generator  $G(E(x))$ , and a discriminator  $D(x, z)$  serves as a baseline that is most similar to the VAE.  $E$  and  $G$  are jointly trained to solve a  $\min_{G, E} \max_D$  optimization problem (we refer to [44] for details on the optimization procedure). We optimized the threshold for the anomaly score to classify NLOS based on a balanced ratio between true positive and true negative on the validation data set.

2) *Performance evaluation*: We train the VAE using the MSE and derive the anomaly score for all the CIRs in the test dataset. We estimated the hyperparameter  $\beta$  experimentally and found that  $\beta = 10^{-3}$  yields stable results for both environments. Fig. 4 shows a histogram of anomaly scores of the test dataset using the TISSI as evaluation metric. Note that as TISSI is not a distance metric, lower values indicate more anomalous signals, while higher values are less anomalous. It is clearly visible that NLOS signals yield a lower TISSI anomaly score than (most of) the LOS signals.

<sup>3</sup>We searched in the following range  $\nu \in \{0, \dots, 1\}$ ,  $\Gamma \in \{10^{-1}, \dots, 10^{-5}\}$ , kernels = {linear, radial} and selected the best parameters based on the test data. For training with clean dataset: {kernel='lin',  $\nu = 0.54$ }; for the corridor dataset: {kernel='lin',  $\nu = 0.77$ }

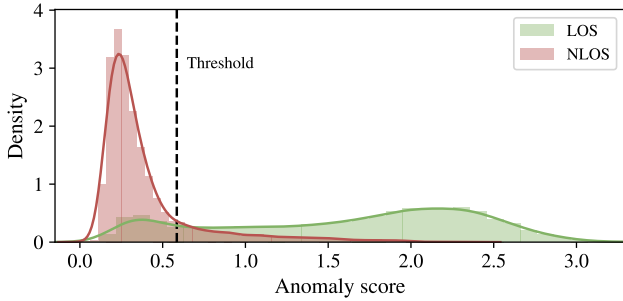


Fig. 4: Anomaly scores histogram (TISSI), trained with MSE.

TABLE I: Performance of the proposed algorithm and the baselines trained in the Clean|Corridor scenario. The algorithms are evaluated in the Corridor environment.

	ACC	F1	PREC	LOS	NLOS
VAE	0.85 0.85	0.85 0.85	0.85 0.85	0.85 0.85	0.84 0.85
GAN	0.79 0.81	0.79 0.81	0.79 0.81	0.79 0.81	0.79 0.81
OC-SVM	0.79 0.80	0.79 0.79	0.79 0.85	0.76 0.61	0.83 0.99
GMM	— 0.81	— 0.81	— 0.81	— 0.83	— 0.79
CORR	0.67 0.69	0.67 0.69	0.67 0.69	0.67 0.69	0.67 0.69

We can also easily derive the appropriate threshold, i.e., in this case at 0.58, which yields a classification accuracy of 85%. Trained also on LOS CIRs from the corridor scenario the accuracy remains the same. This not only proves that the VAE captures environment-specific properties of the LOS CIRs, it also shows that the VAE generalizes well to different unseen environments and propagation conditions as the accuracy remains the same.

Table I shows the results of our VAE along with the results of the baseline algorithms trained in the clean and in the corridor environment, respectively. Our VAE-based model outperforms all baselines. The non ML-based approach (CORR) lacks far behind (67% accuracy in the clean scenario and 69% in the corridor). While, OC-SVM (79% and 80%) and GMM perform similarly well, GMM can only be trained in a mixed environment as both classes (LOS and NLOS) are needed for training. For GMM we used a subset of the corridor scenario for training. While the aforementioned approaches have the same accuracy, the OC-SVM overfits to NLOS with a recall of 83% trained in the clean and 99% in the corridor environment.

We see several limitations of the ML-based baselines. First, there is an information loss induced by the manual feature extraction. Second, the complexity of the decision boundary is limited by the underlying model (OCSVM: restricted to decision boundaries provided by kernels; GMM: assumes that the features are normally distributed for each class). The OC-SVM needs a labeled dataset with LOS and NLOS samples to tune the hyper-parameters (which is also difficult as the algorithm is very sensitive to hyperparameter changes).

However, their most important limitation stems from the lack of generality of the employed features as many multipath-related features may have similar outcomes under different

propagation conditions in other environments.<sup>4</sup>

For the non ML-based baseline (CORR) that estimates a continuous reliability score we also choose a threshold with an equal recall ratio. However, the overall accuracy is low compared to the other approaches, which means that the reference CIRs are only a rough representation of the LOS distribution within the environments.

The GAN yields an accuracy of 79% for the clean environment and 81% for the corridor environment. While this potentially can be further tuned and optimized (even to be *en par* with the VAE) we experienced stability issues during training (which is a known challenge [39]) as the optimization is very sensitive to hyperparameters.

3) *Metric evaluation*: We proposed three different metrics to model the log-likelihood of the CIRs in the VAE. For this, we again evaluate the performance of the metrics using training and test data from the corridor environment. While we use all metrics for the evaluation, we trained our model only with the MSE metric.

The accuracies range from 77% using the MSE, to 82% for the PEAR and up to 85% for the TISSI metric. The MSE for evaluation performs worst, which indicates that the MSE is able to serve the VAE in the modeling of the data distribution but fails to evaluate the semantic similarity of the data. However, compared to the generic time-series metrics, TISSI yields the highest accuracies for the evaluation as the metric is specified to measure the application-specific properties of the CIR.

## B. EKF Tracking integration

A TOF-based EKF expects unbiased range estimates with Gaussian distributed errors. Our idea is to use the estimated anomaly score  $\Psi_n$  to determine a bias  $b(\Psi_n)$  and variance  $\sigma^2(\Psi_n)$  for every receiver  $n$  and range estimation.

With a second dataset that contains ranging errors and corresponding CIRs we first estimate the anomaly score of every CIR and then bin the ranging errors based on the anomaly scores, see Fig. 5. We split the dataset into 14 bins with uniform sizes and exclude bins with small sample counts. The red dots show the mean ranging error, while the vertical lines show the standard deviation within the bins. There is a

<sup>4</sup>For instance, the energy level of LOS CIRs in multipath-free propagation can have the same value range as NLOS CIRs under conditions with multipath due to constructive interference. However, as we may have not seen the NLOS CIRs in the target environment during training, the ML based models mistakenly classify such CIRs as LOS.

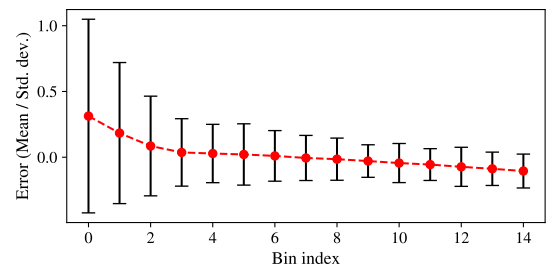
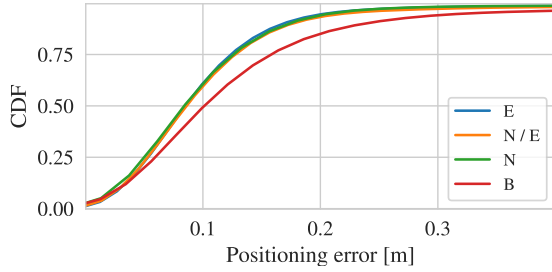


Fig. 5: Ranging error [m] binned using the anomaly score (red dots: bin's mean bias; black lines: bin's standard deviation).



**Fig. 6:** Localization error as CDF with NLoS detection (N), with error correction only correcting NLoS signals (N/E), only error correction (E), and a baseline (B) without correction.

clear correlation between mean ranging error and the anomaly score. The mean ranging error increases monotonically with smaller TISSI, and the standard deviation (thus also the variance) increases with a higher reconstruction error, which indicates the degradation of the range estimation with low quality signals. During tracking we estimate an anomaly score for every receiver and determine the corresponding bin to get the mean bias and variance of the anomaly category. We also use the proposed NLOS identification approach to determine the channel state of the signals (LOS / NLOS). For this experiment we use a trajectory from the corridor scenario separated from the training dataset.

Fig. 6 shows the cumulative distribution function (CDF) of the localization error using the bias and variance estimation (E), a combination of NLOS identification and bias variance estimation where we only correct the TOFs from the NLOS signals (N/E), an estimator that simply excludes detected NLOS signals (N), and a baseline (B) that uses all CIRs for tracking without any correction. Table II shows the mean absolute error (MAE) where *Clean* means that the VAE is trained on LOS CIRs of the clean scenario and *Corridor* that the VAE is trained using LOS CIRs from the corridor scenario. From the results we can clearly see that our anomaly score significantly improves the tracking performance. While simply excluding NLOS signals (N) already improves the localization error of 13.7 cm (without any correction) by about 25 % to 10.3 cm. We also achieve similar results of 10.8 cm by reusing all receivers if we use the bias and variance estimation (E).

However, reusing NLOS signals (N/E) and only applying the variance and bias estimation to them does not improve the localization error over E. The high variance of the NLOS ranging errors leads to a low influence of the NLOS links in the EKF compared to the LOS signals with a significantly lower variance. By using the VAE trained on the corridor scenario, the localization performance slightly increases for the error

**TABLE II:** MAE in the Corridor scenario by using the VAE trained with LOS CIRs of the clean and corridor scenario.

Variant	MAE [m] (Clean)	MAE [m] (Corridor)
E	0.109	0.101
N/E	0.108	0.106
N	0.103	0.103
B	0.137	0.137

correction E. By using scenario-specific LOS signals from the corridor environment, the VAE can take the predominant propagation conditions into account to model the reliability more accurate. The NLOS identification accuracy remains the same for both environments, thus also the tracking performance by excluding NLOS signals N. However, the overall performance is quite similar for our approach trained in both environments, which indicates that the proposed algorithm generalizes well to different environments and propagation conditions.

Note that while we also could have trained a regression model to predict a bias and variance from an anomaly score we resort to the simple binning scheme to better analyze and evaluate the tracking performance of our EKF.

## VI. CONCLUSION

We presented a channel quality estimation approach based on out-of-distribution detection with VAEs. In contrast to previous work we only need LOS training data to yield a high level of generalization. Through the modelling of the distribution of reliable LOS CIRs we derive an anomaly score that enables a deep integration into classical tracking filters such as TOF-based EKFs. The reliability score extracted through an application-specific metric TISSI predicts NLOS CIRs with an accuracy of 85 %, trained in a pure LOS environment and can be used to estimate the bias and variance of TOF estimates, improving the tracking performance by over 25 %.

## REFERENCES

- [1] T. Koike-Akino, P. Wang, M. Pajovic, H. Sun, and P. V. Orlik, "Fingerprinting-based indoor localization with commercial mmwave wifi: A deep learning approach," *IEEE Access*, vol. 8, pp. 79–92, 2020.
- [2] C. Zhou, J. Yuan, H. Liu, and J. Qiu, "Bluetooth indoor positioning based on rssi and kalman filter," *Wireless Personal Comm.*, vol. 96, no. 3, pp. 4115–4130, 2017.
- [3] H. Xu, M. Wu, P. Li, F. Zhu, and R. Wang, "An rfid indoor positioning algorithm based on support vector regression," *Sensors J.*, vol. 18, no. 5, p. 1504, 2018.
- [4] G. Mendoza Silva, J. Torres-Sospedra, and J. Huerta, "A meta-review of indoor positioning systems," *Sensors J.*, vol. 19, p. 4507, 2019.
- [5] D. Dardari, A. Conti, U. Ferner, A. Giorgetti, and M. Z. Win, "Ranging with ultrawide bandwidth signals in multipath environments," *Proc. of the IEEE*, vol. 97, no. 2, pp. 404–426, 2009.
- [6] K. Yu, K. Wen, Y. Li, S. Zhang, and K. Zhang, "A novel nlos mitigation algorithm for uwb localization in harsh indoor environments," *IEEE Trans. Vehicular Technology*, vol. 68, no. 1, pp. 686–699, 2018.
- [7] M. Stahlke, S. Kram, C. Mutschler, and T. Mahr, "Nlos detection using uwb channel impulse responses and convolutional neural networks," in *Intl. Conf. Localization and GNSS (ICL-GNSS)*, 2020.
- [8] S. Kram, M. Stahlke, T. Feigl, J. Seitz, and J. Thielecke, "UWB channel impulse responses for positioning in complex environments: A detailed feature analysis," *Sensors J.*, vol. 19, no. 24, p. 5547, 2019.
- [9] Z. Miao, L. Zhao, W. Yuan, and F. Jin, "Application of one-class classification in nlos identification of uwb positioning," in *Intl. Conf. Information System and Artificial Intelligence (ISAI)*, pp. 318–322, 2016.
- [10] M. Kolakowski and J. Modelski, "First path component power based NLOS mitigation in UWB positioning system," in *Telec. Forum*, 2017.
- [11] Weijie Li, Tingting Zhang, and Qinyu Zhang, "Experimental researches on an UWB NLOS identification method based on machine learning," in *IEEE Intl. Conf. Comm. Technology*, pp. 473–477, 2013.
- [12] A. Ardiansyah, G. Nugraha, H. Han, C. Deokjai, S. Seo, and J. Kim, "A decision tree-based nlos detection method for the uwb indoor location tracking accuracy improvement," *Intl. J. Comm. Systems*, p. e3997, 2019.
- [13] Z. Liu, M. Yang, C. Xu, and H. Yu, "A novel ultra-wideband-based localization and tracking scheme with channel classification," in *IEEE Vehicular Technology Conf. (VTC Spring)*, 2017.

- [14] V. Barral, C. Escudero, J. García-Naya, and R. Maneiro-Catoira, "Nlos identification and mitigation using low-cost uwb devices," *Sensors J.*, vol. 19, p. 3464, 2019.
- [15] A. Niitsoo, T. Edelhäuser, E. Eberlein, N. Hadaschik, and C. Mutschler, "A deep learning approach to position estimation from channel impulse responses," in *Sensors J.*, 2019.
- [16] A. Niitsoo, T. Edelhäuser, and C. Mutschler, "Convolutional neural networks for position estimation in tdoa-based locating systems," in *Intl. Conf. Indoor Positioning and Indoor Navigation*, 2018.
- [17] T. Feigl, S. Kram, P. Woller, R. Siddiqui, M. Philippsen, and C. Mutschler, "A bidirectional lstm for estimating dynamic human velocities from a single imu," in *Intl. Conf. Indoor Positioning and Indoor Navigation*, (Pisa, Italy), 2019.
- [18] K. Cwalina, P. Rajchowski, O. Blazkiewicz, A. Olejniczak, and J. Sadowski, "Deep learning-based los and nlos identification in wireless body area networks," *Sensors J.*, vol. 19, p. 4229, 2019.
- [19] F. Wang, Z. Xu, R. Zhi, J. Chen, and P. Zhang, "Los/nlos channel identification technology based on cnn," in *Conf. Information and Comp. Sc.*, (Hanoi, Vietnam), pp. 200–203, 2019.
- [20] C. Jiang, J. Shen, S. Chen, Y. Chen, D. Liu, and Y. Bo, "Uwb nlos/los classification using deep learning method," *IEEE Comm. Letters*, vol. 24, no. 10, pp. 2226–2230, 2020.
- [21] J. Park, S. Nam, H. Choi, Y. Ko, and Y.-B. Ko, "Improving deep learning-based uwb los/nlos identification with transfer learning: An empirical approach," *Electronics*, vol. 9, no. 10, 2020.
- [22] Z. Zeng, R. Bai, L. Wang, and S. Liu, "Nlos identification and mitigation based on cir with particle filter," in *IEEE Wireless Comm. and Networking Conference (WCNC)*, pp. 1–6, IEEE, 2019.
- [23] J. Fan and A. S. Awan, "Non-line-of-sight identification based on unsupervised machine learning in ultra wideband systems," *IEEE Access*, vol. 7, pp. 32464–32471, 2019.
- [24] S. Marañón, W. M. Gifford, H. Wymeersch, and M. Z. Win, "NLOS identification and mitigation for localization based on UWB experimental data," *J. Sel. Areas in Comm.*, vol. 28, no. 7, pp. 1026–1035, 2010.
- [25] Q. Zhang, D. Zhao, S. Zuo, T. Zhang, and D. Ma, "A low complexity nlos error mitigation method in uwb localization," in *IEEE Intl. Conf. Comm. in China (ICCC)*, 2015.
- [26] H. Wymeersch, S. Marañón, W. M. Gifford, and M. Z. Win, "A machine learning approach to ranging error mitigation for uwb localization," *IEEE Trans. Comm.*, vol. 60, no. 6, pp. 1719–1728, 2012.
- [27] T. Wang, K. Hu, Z. Li, K. Lin, J. Wang, and Y. Shen, "A semi-supervised learning approach for uwb ranging error mitigation," *IEEE Wireless Comm. Letters*, vol. 10, no. 3, pp. 688–691, 2021.
- [28] L. Schmid, D. Salido-Monzú, and A. Wieser, "Accuracy assessment and learned error mitigation of uwb tof ranging," in *Intl. Conf. Indoor Positioning and Indoor Navigation (IPIN)*, (Pisa, Italy), 2019.
- [29] K. Bregar and M. Mohorčič, "Improving indoor localization using convolutional neural networks on computationally restricted devices," *IEEE Access*, vol. 6, pp. 17429–17441, 2018.
- [30] A. Venus, E. Leitinger, S. Tertinek, and K. Witrisal, "Reliability and threshold-region performance of toa estimators in dense multipath channels," in *Intl. Conf. Comm. Workshops*, pp. 1–7, 2020.
- [31] S. Mazuelas, A. Conti, J. C. Allen, and M. Z. Win, "Soft range information for network localization," *IEEE Trans. on Signal Processing*, vol. 66, no. 12, pp. 3155–3168, 2018.
- [32] C. Mao, K. Lin, T. Yu, and Y. Shen, "A probabilistic learning approach to uwb ranging error mitigation," in *IEEE Global Comm. Conf.*, 2018.
- [33] V. Chandola, A. Banerjee, and V. Kumar, "Anomaly detection: A survey," *ACM computing surveys (CSUR)*, vol. 41, no. 3, pp. 1–58, 2009.
- [34] R. Chalapathy, A. Menon, and S. Chawla, "Anomaly detection using one-class neural networks," *arXiv:1802.06360v2 [cs.LG]*, 2019.
- [35] P. Oza and V. Patel, "One-class convolutional neural network," *IEEE Signal Processing Letters*, vol. PP, pp. 1–1, 2018.
- [36] I. J. Goodfellow, J. Pouget-Abadie, M. Mirza, B. Xu, D. Warde-Farley, S. Ozair, A. C. Courville, and Y. Bengio, "Generative adversarial nets," in *Conf. Neural Information Proc. Sys.*, pp. 2672–2680, 2014.
- [37] H. Zenati, C. S. Foo, B. Lecouat, G. Manek, and V. R. Chandrasekhar, "Efficient gan-based anomaly detection," 2019.
- [38] S. Akcay, A. Atapour-Abarghouei, and T. P. Breckon, "GANomaly: Semi-supervised Anomaly Detection via Adversarial Training," in *Computer Vision - Asian Conf. on Computer Vision (ACCV)*, (Cham), pp. 622–637, 2019.
- [39] M. Arjovsky and L. Bottou, "Towards principled methods for training generative adversarial networks," *Intl. Conf. for Learning Representations (ICLR)*, 2017.
- [40] J. An and S. Cho, "Variational autoencoder based anomaly detection using reconstruction probability," tech. rep., Seoul National Univ., 2015.
- [41] D. P. Kingma and M. Welling, "Auto-encoding variational bayes," in *Intl. Conf. Learning Representations (ICLR)*, 2014.
- [42] I. Higgins, L. Matthey, A. Pal, C. P. Burgess, X. Glorot, M. Botvinick, S. Mohamed, and A. Lerchner, "beta-vae: Learning basic visual concepts with a constrained variational framework," in *ICLR*, 2017.
- [43] T. W. Liao, "Clustering of time series data—a survey," *Pattern recognition*, vol. 38, no. 11, pp. 1857–1874, 2005.
- [44] H. Zenati, C. Foo, B. Lecouat, G. Manek, and V. Chandrasekhar, "Efficient gan-based anomaly detection," *arXiv:1802.06222*, 2019.



**Maximilian Stahlke** received his Master's degree in Electronic and Mechatronic Systems at the Institute of Technology Georg Simon Ohm, Germany, in 2020. Since 2020 he works at the Locating and Communication Systems department at Fraunhofer IIS in the Machine Learning & Information Fusion group. His research interests are hybrid positioning for radio-based localization systems with the focus on model- and data-driven sensor fusion.



**Sebastian Kram** received his MSc. degree in Electrical and Communication Engineering at the FAU Erlangen-Nürnberg in 2017. He then joined the Locating and Communication Systems department at Fraunhofer IIS. Since 2020 he is also working in the Navigation Group at the Chair for Information Technology (Communication Electronics) at FAU. He focuses on radio signal-based adaptive cooperative positioning using both model- and data-driven methods.



**Felix Ott** received his MSc. degree in Computational Engineering at the FAU Erlangen-Nürnberg in 2019. He joined the Hybrid Positioning & Information Fusion group in the Locating and Communication Systems department at Fraunhofer IIS. In 2020 he started his Ph.D. at the Ludwig-Maximilians University in Munich at the Statistical Learning and Data Science chair. His research covers multimodal information fusion for camera- and IMU-based localization.



**Tobias Feigl** is a research associate at the Fraunhofer Institute for Integrated Circuits (IIS) in Nürnberg, Germany and a Ph.D. candidate at the (FAU) Erlangen-Nürnberg, Germany. His research covers the areas of Augmented and Virtual Reality, human-computer interaction, and machine learning. He improves human motion behavior in immersive virtual environments with inertial and radio sensors.



**Christopher Mutschler** leads the precise positioning and analytics department at Fraunhofer IIS. Prior to that, Christopher headed the Machine Learning & Information Fusion group. He gives lectures on machine learning at the FAU Erlangen-Nürnberg (FAU), from which he also received both his Diploma and PhD in 2010 and 2014 respectively. Christopher's research combines machine learning with radio-based localization.